8.3 SCALES OF TURBULENCE DECAY FROM OBSERVATIONS AND DIRECT NUMERICAL SIMULATION

William J. Shaw* and James C. Barnard
Pacific Northwest National Laboratory
Richland, Washington

1. INTRODUCTION

The problem of turbulence decay in the atmospheric boundary layer has not been extensively studied because of the observational and computational difficulties associated with the inherent non-stationarity of the process. Two previous studies (Nieuwstadt and Brost(1986; hereafter NB) and Sorbjan 1997), both based on large-eddy simulation, have proposed velocity and time scales for turbulence variables during the decay process associated with the afternoon transition from daytime convective conditions to nocturnal stable stratification. The study by NB was quite idealized and used large-eddy simulation (LES) to model the response of a convective boundary layer with zero wind to an abrupt shut-off of surface heat flux. Among other results, NB found that appropriate length and velocity scales for the decaying turbulence were the depth *h* of the boundary layer and the convective velocity scale $w_* = \left(g\overline{w'\theta'}h/T_o\right)^{1/3}$, which can be combined to provide a time scale t_* for the decay process. Sorbjan performed a similar but more realistic study by having the surface heat flux diminish as a quarter sinusoid. For decay under these conditions, he found that a second time scale τ_f, the time between maximum and zero heat flux, was also important. In addition to zero wind, both of these studies simulated conditions in which the boundary layer depth remained constant as turbulence decayed.

In October 2000, as part of its Vertical Mixing (VTMX) initiative, the Environmental Meteorology Program of the U.S. Department of Energy carried out an extensive field campaign in the Salt Lake Valley of Utah. An overall goal was to improve our understanding of transport and mixing processes, particularly in stably stratified and transitional periods and in urban basins or valleys. As part of that study, we have collected data from a sonic anemometer, a minisodar, and a 915 MHz wind profiling radar that were located near the center of the valley. In this paper, we use turbulence measurements from the sonic anemometer and the wind profiling radar to explore the behavior of these scales in a real atmospheric boundary layer. We also compare the previous scaling results and results from the observations with direct numerical simulations (DNSs) of turbulence driven by both idealized and observed time series of surface heat flux. The simulations allow us to calculate ensemble averages of turbulence variables and to determine the sensitivity of scales to the particular functional form of the surface heat flux.

*Corresponding author address: Will Shaw, Pacific Northwest National Laboratory, PO Box 999, MS K9-30, Richland, WA 99352; e-mail: will.shaw@pnl.gov.

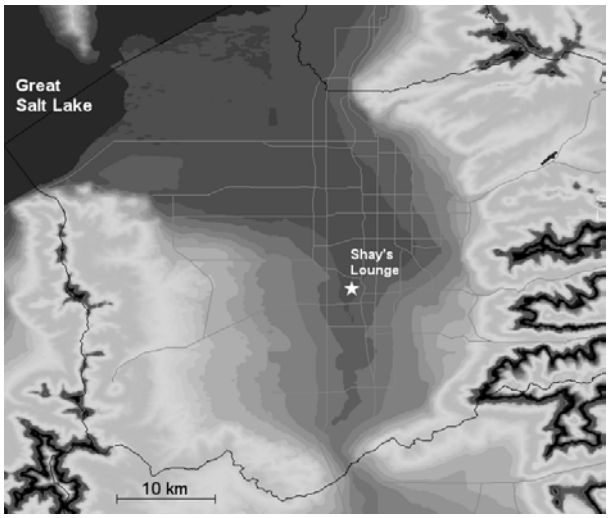

Figure 1. Salt Lake Valley, showing location at which data discussed in this paper were collected.

2. FIELD MEASUREMENTS

Figure 1 shows the location within the Salt Lake Valley at which the observations for this study were made. The site was very near the Jordan River and was at an elevation of 1300 m MSL. For at least 10 km in all directions, the terrain varies relatively gently. To the east, the Wasatch Mountains are approximately 10 km away. The Oquirrh Mountains lie a similar distance to the west. The valley slopes up to the south and is interrupted by the east-west-oriented Traverse Range, which is broken by the Jordan River. From the measurement site, the valley descends gently to Great Salt Lake (elevation 1280 m MSL), approximately 25 km to the north-northwest. The general surrounding of the site might best be described as suburban. The vegetation of the fetch to the north, which was upwind for days that were dominated by regional diurnal circulation, was primarily grasses and forbs <1 m high and scattered trees roughly 3–4 m in height. In other directions was a combination of scattered buildings, city streets, and widespread grasses and trees.

The sonic anemometer was mounted on a small tower 8.5 m AGL, and provided virtual temperature and winds at a sampling rate of 10 s^{-1}. We operated the wind profiler in two modes: five beams with a range gate resolution of 60 m and five with a resolution of 200 m. The profiler sampled in RASS mode for five minutes every half hour. We recorded spectral data from the

profiler for the entire field program.

Data from the sonic anemometer were processed to yield first and second statistical moments and dissipation rate over half-hour averaging periods. We used linear detrending as a high-pass filter. The dissipation rate was calculated from the inertial subrange of velocity spectra.

In defining the structure of the boundary layer, we have found the low mode of the wind profiler to be the most useful. We processed the profiler data using the NCAR Improved Moment Algorithm (NIMA; Morse et al. 2002, Cornman et al. 1998), which employs a combination of pattern recognition and fuzzy logic to extract moments from Doppler spectral peaks. The better peak selection by this method makes feasible the computation of winds over periods as short as 5 min. We have also calculated dissipation rate from the profiler. To obtain these profiles, we have used spectral width data derived from NIMA processing and followed the method described by White et al. (1999) to relate spectral width to dissipation via the structure function. We have corrected for shear broadening effects following Gossard et al. (1998).

3. DIRECT NUMERICAL SIMULATION

Because remote sensing devices such as the wind profiler cannot fully characterize even a stationary, horizontally homogeneous boundary layer, we are also using direct numerical simulation (DNS) to model the turbulent flow as a complementary approach in this investigation. DNS offers one prominent advantage over other models for our purposes: it is a full simulation of eddies at all scales in the flow. There are no parameterizations of the turbulence. The cost is that the simulations must be run at very low Reynolds numbers. Typically $Re \simeq 500$ for DNS in contrast to atmospheric values of O(10^7). Coleman (1999) showed that Reynolds number similarity (that is, independence) seems to begin at Reynolds numbers as low as 400, which means that we have good reason to hope that DNS can faithfully characterize many atmospheric features. Further, de Bruyn Kops and Riley (1998) demonstrated excellent correspondence between DNS and measurements in laboratory flows with matched Reynolds numbers.

The DNS model that we are using was developed by Barnard (2000) and simulates an Ekman layer over flat terrain. It uses 48x48 nodes in the horizontal and 55 in the vertical. Horizontal boundary conditions are periodic, and the bottom boundary conditions can be varied to allow, for example, driving the model with an observed heat flux (that has been suitably scaled). The model can also simulate a boundary layer with a mean wind by the imposition of a horizontal pressure gradient.

Figure 2 shows a comparison between the results for NB's and Sorbjan's surface forcing and the DNS for the decay of domain integrated turbulence kinetic energy (TKE). The DNS was run using the same prescribed surface heat fluxes as in those two studies and with zero mean wind. As one would expect, and as Sorbjan found, turbulence decays more rapidly when heat flux is shut off abruptly than when it diminishes

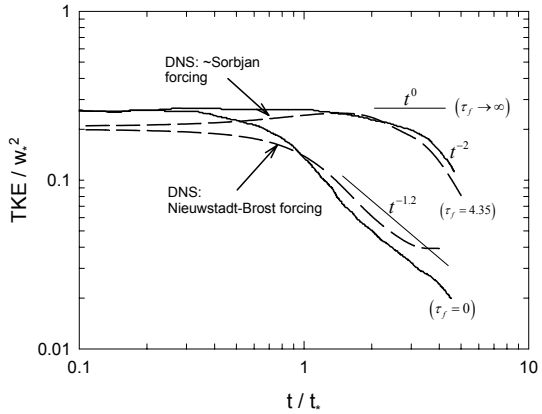

Figure 2. Comparison of evolution of scaled TKE from LES studies of Nieuwstadt and Brost (1986) and Sorbjan (1997) compared with similarly forced DNS. (after Sorbjan's figure).

gradually. The agreement between the LESs and the DNS runs is quite encouraging.

4. THE REAL BOUNDARY LAYER

The real atmospheric boundary layer, particularly over the variable terrain of the Salt Lake Valley, is considerably more complicated than the idealizations described above. For conditions of significant synoptic-scale pressure gradients, the concept of an afternoon decay of turbulence is probably of limited usefulness. However, many days in the October 2000 field program in fact had weak synoptic forcing. In this case, solar heating of the terrain generated regular up-valley flows, with down-valley flows occurring from radiational cooling at night. Figure 3 shows a typical example, with a reversal of wind direction from southerly (down-valley) to north-northwesterly in the late morning, followed by increasing wind speed in the afternoon. This is consistent with a thermally driven circulation "spinning up" during the day. This circulation continues until surface heat flux diminishes to near zero in the late afternoon. The effect of the thermally driven circulation on the near-surface behavior of the turbulence is shown in Figure 4. Here the shear production maintains TKE well past the time it would otherwise have decayed.

We have used the DNS to see what effect the mean wind has on the turbulence decay process in the boundary layer as a whole. Figure 5 shows the scaled volume-integrated TKE as a function of normalized time for simulations driven by observed heat flux. In the first case, decay was simulated with zero wind, and its behavior is very similar to that found by Sorbjan for a quarter-sinusoid roll-off in heat flux. In the second case, a mean wind was applied, and two differences are immediately evident. The decay time is significantly longer when wind is present, and the overall level of TKE scaled by w_* is greater. The longer decay time is expected, since shear production would contribute to the TKE. That TKE no longer scales with w_* is also not surprising, since w_* accounts only for production of TKE by buoyancy forces. Also included in Figure 5 is

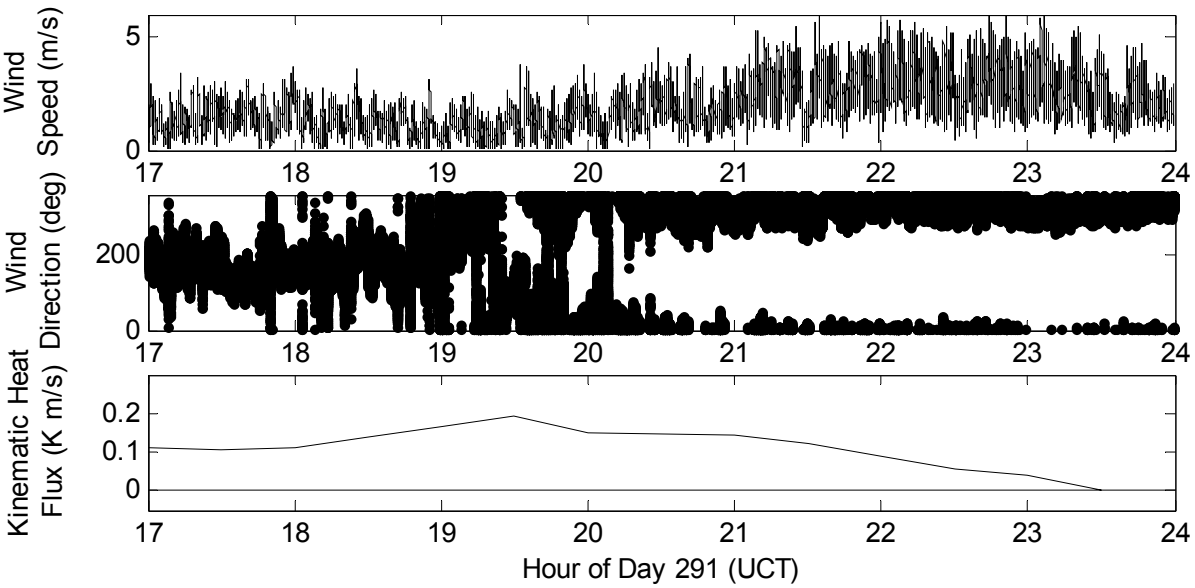

Figure 3. Time series of showing diurnal reversal of flow in the Salt Lake Valley and the associated surface heat flux on 17 October 2000. Note that the wind speed is significant as the heat flux drops toward zero.

the curve of scaled TKE from the sonic anemometer. In this case, the fall-off in TKE does not occur until much later than the DNS indicates. This curve is not completely comparable to the other two, since it represents a point measurement near the surface rather than a volume average of TKE. However, it is consistent. The DNS TKE falls off most rapidly with zero wind and less rapidly when wind is present. Since the effect of shear production is strongest near the surface, the observations reasonably fall off the most slowly.

The profiler provides a view of the evolution of turbulence in the boundary layer. In a pilot study on the Hanford Site (near Pacific Northwest National Laboratory), we compared dissipation measured at the profiler's lowest range gate with that from a sonic anemometer at 120 m on a nearby tower. The agreement was quite good. We have also compared dissipation measured from the sonic anemometer with that from the lowest range gate of the profiler for the same day as Figs. 3 and 4. The variability of dissipation during the day is similar from the two instruments, and the sonic value is higher—which is expected near the surface. Fig. 6 shows a time-height cross section of dissipation rate indicating largest values near the

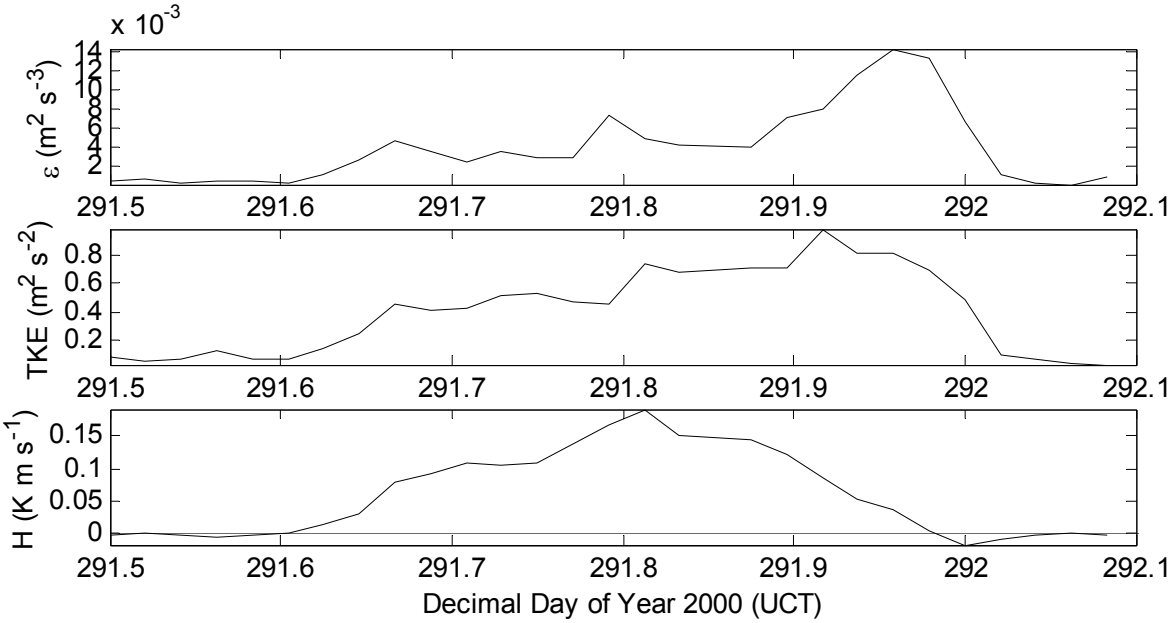

Figure 4. Time series of dissipation rate and TKE with surface heat flux on 17 October. Surface heat flux dropped toward zero much sooner than the other two variables, reflecting the influence of wind shear on turbulence decay.

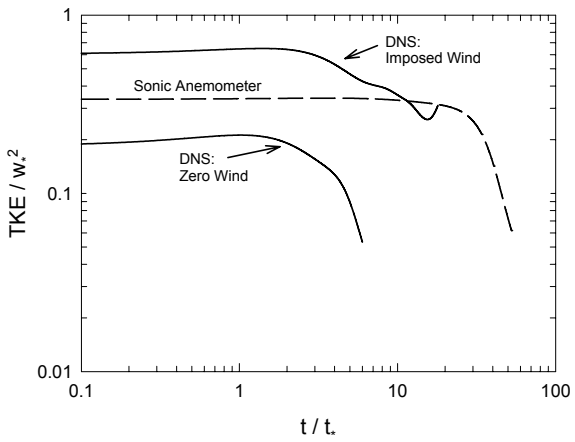

Figure 5. As in Figure 2, but for forcing by observed heat flux with and without wind.

surface and a general growth and decay during the diurnal heating cycle.

Also shown in Figure 6 is boundary layer depth derived from the range-corrected signal-to-noise ratio of the profiler. This rapid increase in mixed layer depth in the morning and comparably rapid decrease in depth in the afternoon was typical of the light-wind days of the VTMX field program. It seems likely that this characteristic of boundary layer evolution is a result of afternoon subsidence over the central Salt Lake Valley that results from the thermally driven circulation.

4. DISCUSSION

We have used a combination of observations and DNS of turbulence to make a preliminary investigation of the decaying turbulence in a real atmospheric boundary layer. Previous efforts at scaling decaying turbulence used large-eddy simulation to address idealized cases with no wind or terrain effects. We have shown that our

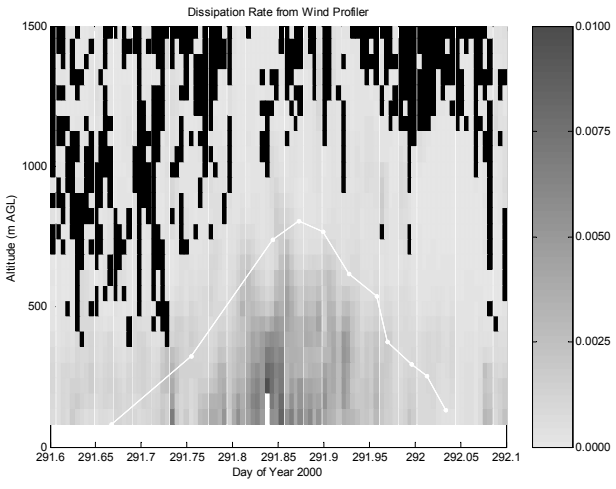

Figure 6. Time-height cross-section of dissipation rate from the wind profiler. Black areas are invalid data, white areas exceed the grayscale. The white line is boundary layer depth from range-corrected SNR.

DNS produces essentially the same results when run for those cases. In a next step, we have driven our DNS with observed time-varying surface heat flux with and without a mean wind. Without wind, results are not very different from Sorbjan's, which use a quarter-sinusoid surface heat flux. With a mean wind, however, shear production substantially extends the decay time of the turbulence. The effect is also evident in the observations of TKE decay from the sonic anemometer. Thus, realistic scaling of the turbulence decay must include an accounting for the shear production of TKE.

Observations of dissipation rate from the profiler show a maximum near the surface with an expected decrease with altitude. This typically occurred, however, within a boundary layer whose depth decreased dramatically in the afternoon. This actual boundary layer behavior differs from the assumption of essentially constant transitional mixed layer depth in the idealized studies and is a reflection of diurnal circulations resulting from sloping terrain and, probably to a lesser extent, large-scale subsidence. As a result, an additional need for developing practical scaling of turbulence decay is to account for effects of changing mixed layer depth. Further exploring these scaling issues is part of our continuing research in the transitional atmospheric boundary layer.

ACKNOWLEDGEMENTS

This work was supported by the U.S. Department of Energy (DOE), under the auspices of the Environmental Meteorology Program of the Office of Biological and Environmental Research. We are grateful to NCAR for providing NIMA to PNNL through a research license and for helpful discussions with Cory Morse of NCAR and Allen White of NOAA. This work was performed at Pacific Northwest National Laboratory, which is operated for DOE by the Battelle Memorial Institute under contract DE-AC0676RLO 1830.

REFERENCES

Barnard, J. C., 2000: Intermittent Turbulence in the Very Stable Ekman Layer. Ph.D. dissertation, Dept. of Mech. Eng., Univ. of Washington.

Coleman, G. N., 1999: Similarity statistics from a direct numerical simulation of the neutrally stratified boundary layer. *J. Atmos. Sci.,* **56**, 891–900.

Cornman, L. B., R. K Goodrich, C. S. Morse, and W. L. Ecklund 1998: A fuzzy logic method for improved moment estimation from Doppler spectra. *J. Atmos. Ocean. Tech.*, **15**, 1287–1305.

De Bruyn Kops, S. M., and J. J. Riley 1998: Direct numerical simulation of laboratory experiments in isotropic turbulence. *Phys. Fluids,* **10**, 2125–2127.

Gossard, E. E., D. E. Wolfe, K. P. Moran, R. A.. Paulus, K. D. Anderson, and L. T. Rogers 1998: Measurement of clear-air gradients and turbulence properties with radar wind profilers. *J. Atmos. Ocean. Tech*., **15**, 321–342.

Morse, C. S., R. K. Goodrich, and L. B. Cornman 2002: The NIMA method for improved moment estimation from Doppler spectra. *J. Atmos. Ocean. Tech*., **19**, 274–295.

Nieuwstadt, F. T. M., and R. A. Brost 1986: The decay of convective turbulence. *J. Atmos. Sci.*, **43**, 532–546.

Sorbjan, Z. 1997: Decay of convective turbulence revisitied. *Bound.-Layer Meteor.*, **82**, 501–515.

White, A. B., R. J. Lataitis, and R. S. Lawrence 1999: Space and time filtering of remotely sensed velocity turbulence. *J. Atmos. Ocean. Tech.*. **16**. 1967–1972.